COMPARISON OF THE T-MATRIX AND HELMHOLTZ INTEGRAL EQUATION METHODS FOR WAVE SCATTERING CALCULATIONS

W. Tobocman

Case Western Reserve University
Physics Department
Cleveland, OH

The T-matrix method (TMM) and the Helmholtz integral equation method (HIEM) are wave scattering formalisms for irregularly shaped targets. They are both based on the Helmholtz integral formula (HIF) but they use different ways to achieve the discretization required for numerical evaluation.

The TMM expands the wave field in a basis function set. Substitution of this expansion into the HIF produces a set of algebraic equations for the expansion coefficients $t_{\ell m}$. We consider acoustic waves in the interest of simplicity. If spherical waves are used as the basis set, then for the case of rigid body scattering we have

$$t_{\ell m} = \sum_{\ell' m'} \{J_{\ell m,\ell' m'} Y_{\ell'}^{m'}(\hat{k}_o)^* + H_{\ell m,\ell' m'} t_{\ell' m'}\} \tag{1a}$$

$$\left\{ \begin{matrix} J_{\ell m,\ell' m'} \\ H_{\ell m,\ell' m'} \end{matrix} \right\} = i^{\ell'-\ell+1} k \oint dS' \, Y_{\ell'}^{m'}(\hat{r}')\hat{n}'\cdot\nabla' Y_{\ell}^{m}(\hat{r}')^* \left\{ \begin{matrix} j_\ell(kr') \\ h_\ell^{(1)}(kr') \end{matrix} \right\} \tag{1b}$$

where the integral is over the surface of the target, $\hat{n}$ is the unit normal, Y is the spherical harmonic , and j and h are the spherical Bessel and Neumann functions, respectively. Eq. (1a) is solved approximately for the $t_{\ell m}$ by truncating the sum on ℓ' at $\ell' = L$ = NPW - 1 and inverting the matrix 1 - H. The scattering amplitude $T(\hat{k})$ is then evaluated as

$$T(\bar{k}) = -\frac{4\pi i}{k} \sum_{\ell m} Y_\ell^m(\hat{k}) t_{\ell m} \tag{2}$$

The HIEM, on the other hand, employs the integral equation for the wave field on the surface of the target

$$\psi(\bar{r}) = 2\psi^{(o)}(\bar{r}) + 2 \oint dS' \; \psi(r') \; \hat{n}'\cdot\nabla' G(\bar{r},\bar{r}') \tag{3a}$$

$$G(\bar{r},\bar{r}') = -\,(4\pi|\bar{r}-\bar{r}'|)^{-1} \exp(ik|\bar{r}-\bar{r}'|) \tag{3b}$$

$$\hat{n}\cdot\nabla\psi(\bar{r}) = 0 \quad \text{(rigid body scattering)} \tag{3c}$$

which follows from the HIF. The integral equation is discretized by dividing the surface of the target into N patches having areas A_α, A_β, A_γ,... and locations $\bar{r}_\alpha$, $\bar{r}_\beta$, $\bar{r}_\gamma$,.... The integral equation is then approximated by

$$\psi(\bar{r}_\alpha) = \psi_\alpha \simeq 2\,\psi_\alpha^{(o)} + 2 \sum_{\beta=1}^{N} K_{\alpha\beta}\psi_\beta \tag{4a}$$

$$K_{\alpha\beta} = A_\beta \, \hat{n}_\beta\cdot\nabla_\beta \, G(\bar{r}_\alpha,\bar{r}_\beta) \qquad \alpha \neq \beta \tag{4b}$$

$$K_{\alpha\alpha} = \int_{A_\alpha} dS \; \hat{n}\cdot\nabla \; G(r_\alpha,r)\,. \tag{4c}$$

This set of algebraic equations is solved by inverting the matrix 1-2K. The solution is then used to evaluate the scattering amplitude by means of

$$T(\bar{k}) = -\frac{i}{4\pi} \sum_{\alpha=1}^{N} A_\alpha\psi_\alpha \; \bar{n}_\alpha\cdot\bar{k} \; \exp(-i\bar{k}\cdot\bar{r}_\alpha)\,. \tag{5}$$

We have carried out a comparison of the two methods by using them both to analyze the same problem, the scattering of a plane wave $\psi^{(o)} = \exp(i\,k\,z)$ by a rigid prolate spheroid. The direction of incidence is taken to be perpendicular to the major axis and the scattered intensity $|T(\bar{k})|$ is calculated in the plane of the major axis and the direction of incidence. We compared, in particular, how rapidly the TMM converged with increasing NPW and how rapidly the HIEM converged with increasing N. Figures 1 through 4 show the results for four different values of the aspect ratio A = a/c. The wave number k and the major axis c of the spheroid were both taken to be unity. The open symbols represent the HIEM results and the solid symbols represent the TMM results.

In Fig. (1) we have the results for a spherical target. We see that the TMM has converged for NPW = 3 while the HIEM requires N = 64 to achieve convergence. So for the spherical case the TMM using the spherical basis set converges more rapidly than the HIEM.

As the number of partial waves NPW employed by the TMM is increased and the dimension of the matrix 1 - H is thereby increased, we find that 1 - H becomes increasingly more ill-conditioned, and finally for a large enough NPW the matrix 1 - H becomes singular or an overflow occurs.

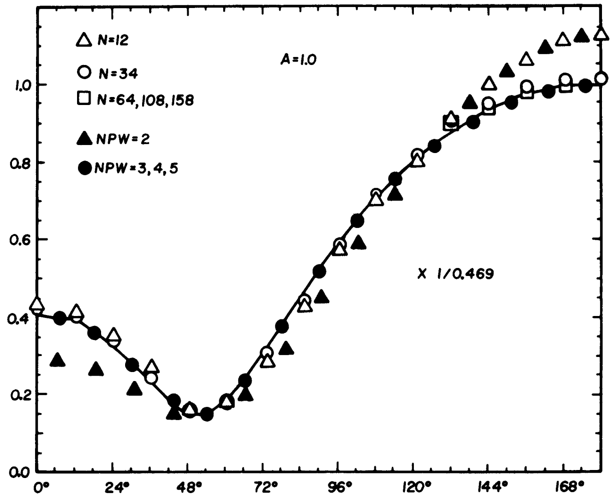

Fig. 1 Scattering amplitude $|T(\theta)|$ as a function of the scattering angle θ for a plane acoustic wave of wavenumber k = 1.0 incident on a rigid prolate spheroid of major semi-axis c = 1.0 and minor semi-axis a = 1.0. The direction of incidence is perpendicular to the axis of symmetry and the scattering plane is that of the symmetry axis and the direction of incidence. The open symbols represent values calculated with the HIEM using N patches. The solid symbols represent values calculated with the TMM using NPW partial waves. The curve is the exact result.

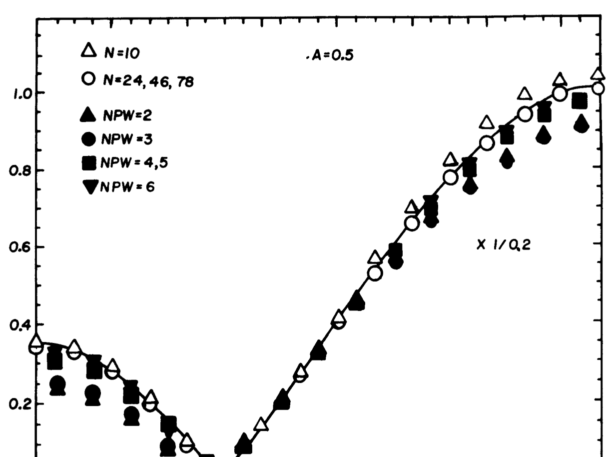

Fig. 2 Same as Fig. 1 except that A = 0.5 and the curve is merely drawn to aid the eye.

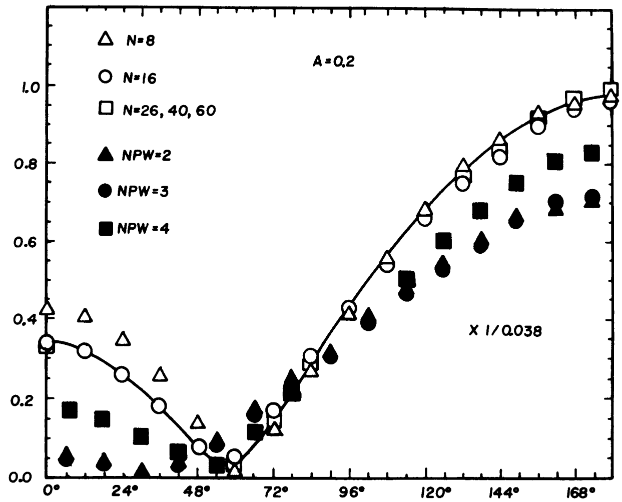

Fig. 3 Same as Fig. 2 except that A = 0.2.

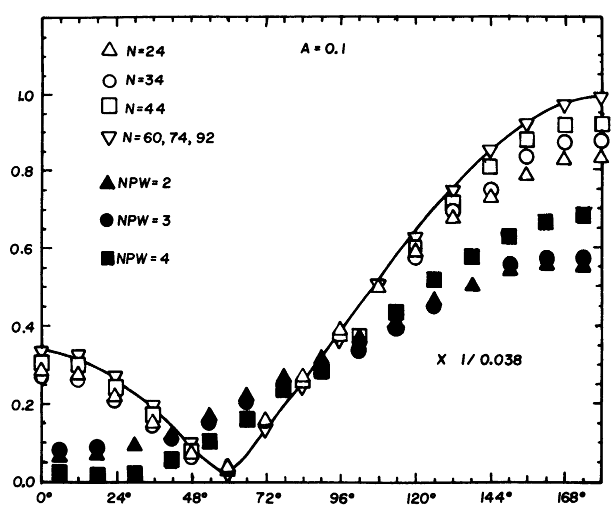

Fig. 4 Same as Fig. 2 except that A = 0.1.

Thus there is an upper limit on NPW. This effect becomes more pronounced as the target shape is made more nonspherical, i.e. as the aspect ratio A departs from the unity to a greater extent. Thus we observe in Figs. (2), (3), and (4) that with decreasing A the approach to convergence for the TMM is halted further and further from the desired values.

Turning now to the HIEM we find that as the number of patches N increases and the dimension of the matrix 1-2K is increased accordingly, the matrix 1-2K becomes better conditioned. Thus in the course of these HIEM calculations we never encountered any overflows or found the matrix 1-2K to become singular. Thus convergence was easily achieved in each of the four cases.

In Tables I, II, III, and IV we display in tabular form the results for forward and backward scattering for a similar set of cases except that the wave number k is 6.0 instead of 1.0. On the tables we display the condition numbers of the matrices to be inverted. For the TMM we also indicate the number of Gaussian quadrature points used in the integration on zenith angle in the evaluation of the matrix elements of J and H. Because of azimuthal symmetry, the azimuthal angle integration could be done in closed form.

Table I

HIEM				a=1.0 k=6.0	TMM			
N	C No.	$\|T(0^o)\|$	$\|T(180^o)\|$	NGP	NPW	C No.	$\|T(0^o)\|$	$\|T(180^o)\|$
12	5.97	1.202	1.269	48	5	1.01	1.796	.6001
34	1.68	4.325	1.987	48	6	1.01	1.844	.1084
64	1.46	2.545	.8494	48	7	317	2.114	.7595
108	1.28	2.344	.3991	48	8	$1.1x10^3$	2.235	.4769
158	1.19	2.316	.5085	56	8	$1.8x10^3$	2.235	.4769
EXACT		2.267	.5309	104	8	$5.0x10^5$	2.235	.4769
				48	9	$6.0x10^7$	2.262	.5399
				48	10	overflow		
						EXACT	2.267	.5309

Table II

HIEM				a=0.5 k=6.0	TMM			
N	C No.	|T(0°)|	|T(180°)|	NGP	NPW	C No.	|T(0°)|	|T(180°)|
10	2.97	1.674	.5991	48	3	1.05	.5322	.4815
24	1.31	1.086	.9565	48	4	1.11	.7297	.3961
46	1.21	1.166	.3570	48	6	2.26	.9845	.7304
78	1.13	1.128	.4651	48	8	8.2×10^3	.9800	.4678
114	1.09	1.120	.4624	56	8	5.6×10^3	1.065	.5567
156	1.07	1.116	.4625	64	8	1.8×10^4	1.65	.4368
				48	9	6.3×10^6	.9979	.4828
				48	10	overflow		

TABLE III

HIEM				a=0.2 k=6.0	TMM			
N	C No.	|T(0°)|	|T(180°)|	NGP	NPW	C No.	|T(0°)|	|T(180°)|
8	1.82	.3940	.3318	104	3	1.67	.1800	.2854
16	1.55	.3525	.5745	104	4	3.92	.2329	.3614
26	1.31	.3660	.5350	72	4	3.92	.2329	.3614
40	1.19	.3699	.4757	64	4	3.92	.2329	.3614
60	1.13	.3711	.5006	104	5	17.5	.2478	.3800
82	1.09	.3705	.5028	104	6	117	.3731	.1441
106	1.07	.3707	.5043	104	7	994	.5373	.3739
134	1.06	.3706	.5047	104	8	1.0×10^4	.3830	.5394
				88	8	1.0×10^4	.8631	.5119
				120	8	1.0×10^4	1.048	.7245
				80	9	1.8×10^8	Overflow	

TABLE IV

HIEM				a=0.1 k=6.0	TMM			
N	C No.	$\|T(0^o)\|$	$\|T(180^o)\|$	NGP	NPW	C No.	$\|T(0^o)\|$	$\|T(180^o)\|$
18	2.60	.1448	.2487	96	2	1.60	.0306	.0993
24	2.01	.1382	.2670	96	3	4.83	.0269	.1356
34	1.62	.1284	.2785	96	4	29.2	.0474	.1780
44	1.43	.1315	.2930	96	5	299	.0411	.1933
60	1.28	.1365	.3018	96	6	4.2×10^3	.2749	.1164
74	1.21	.1368	.3003	96	7	6.7×10^4	.5212	.1928
92	1.61	.1355	.2986	88	7	6.5×10^4	1.481	1.099
114	1.13	.1344	.2967	104	7	6.9×10^4	.9770	.5898
132	1.11	.1348	.2974	88	8	1.7×10^6	Overflow	

The parameters for the Tables are the same as for the corresponding Figures except that k = 6.0. C No. is the condition number and NGP is the number of meshpoints used in the Gaussian quadrature procedure.

We conclude that the HIEM is numerically better adapted than the TMM to the calculation of scattering by irregularly shaped targets. In addition the HIEM will be more efficient for large scale calculations because the required matrix elements are given by algebraic expressions rather than surface integrals and are therefore less time consuming to calculate for nonsymmetrical target shapes.

The author is grateful to Case Western Reserve University for the use of its D.E.C. VAX 11/780 computer.